Supporting Information for:

Electronic and Structural Differences between Wurtzite and Zinc Blende InAs Nanowire Surfaces: Experiment and Theory

Martin Hjort,[1] Sebastian Lehmann,[1] Johan Knutsson,[1] Alexei A. Zakharov,[2] Yaojun A. Du,[3] Sung Sakong,[3] Rainer Timm,[1] Gustav Nylund,[1] Edvin Lundgren,[1] Peter Kratzer,[3] Kimberly A. Dick,[1,4] and Anders Mikkelsen[1]*

[1] *Department of Physics and The Nanometer Structure Consortium, Lund University, P.O. Box 118, 221 00 Lund, Sweden*

[2] *MAX IV-laboratory, Lund University, P.O. Box 118, 221 00 Lund, Sweden*

[3] *Fakultät für Physik and Center for Nanointegration (CENIDE), Universität Duisburg-Essen, Lotharstrasse 1, 470 48 Duisburg, Germany*

[4] *Centre for Analysis and Synthesis, Lund University, P.O. Box 124, 221 00, Lund, Sweden*

[*]e-mail: anders.mikkelsen@sljus.lu.se

Growth details:

For STM, the tip movement is limited by piezo actuators and therefore, the length of each NW crystal segment was designed to be 500 nm in order to easily find areas of interest such as Wz–Zb transitions. For the STM sample 80 nm Au-particles were deposited on InAs(−1−1−1) wafers with an areal density of 1 μm^{-2} using an aerosol technique.[1] For LEEM/PEEM the position of Au-particles on the InAs(−1−1−1) wafer was patterned using electron-beam lithography (EBL) in a Raith 150 setup with an equivalent areal density of 4 μm^{-2} and each crystal segment was grown to be about 1 μm long which is suitable for the PEEM and LEEM studies. Both NW samples were grown at a temperature of 460°C using arsine (AsH_3) and trimethylindium (TMIn) as

precursors at total reactor flows of 13 slm, and a total reactor pressure of 100 mbar. For the STM sample, the molar fractions were set to $\chi_{TMIn} = 3.5\times10^{-6}$ while those for AsH_3 were adjusted to $\chi_{AsH3} = 1.5\times10^{-3}$ and $\chi_{AsH3} = 3.6–2.3\times10^{-5}$ for Zb and Wz, respectively. For the LEEM/PEEM sample, the molar fractions were slightly different in order to compensate for the different NW density, and set to $\chi_{TMIn} = 5.2\times10^{-6}$ while those for AsH_3 were set to $\chi_{AsH3} = 3.6\times10^{-3}$ and $\chi_{AsH3} = 1.9\times10^{-5}$ for Zb and Wz, respectively. In order to remove the surface oxides and allow proper surface preconditioning, a 7 min annealing step was carried out prior to growth at a maximum temperature of 550 °C in AsH_3/H_2 atmosphere. After that step the temperature was reduced to growth temperature, and after thermal stabilization the precursors were introduced to initiate the growth.

STM experimental details:

Electrochemically etched tungsten tips that had been cleaned and sharpened in vacuum by Ar-ion sputtering were used. For STS point spectra, the tip was placed at an area of interest and $I-V$ and $(dI/dV)-V$ spectra were recorded simultaneously. For the $(dI/dV)-V$ measurements, showing the differential conductivity, a lock-in amplifier was used with modulation amplitude V_{mod} = 80 mV, and modulation frequency f_{mod} = 1.1 kHz. To increase the dynamic range of the STS measurements at the band edges, the tip–sample separation was decreased with decreasing absolute value of the sample bias by ~2 Å/V, according to the variable gap mode.[2, 3] The obtained $(dI/dV)-V$ curves were normalized to the total conductance ($I-V$) broadened by convolution with an exponential function, as presented in Ref.[2], using a broadening width of 0.5–1.5 V. The final curve showing $((dI/dV) / \overline{(I/V)} - V$ depicts a quantity that is proportional to the local density of states (LDOS).[4, 5]

PEEM/LEEM experimental details:

All experiments were performed using an electron energy analyzer measuring the number of electrons as a function of kinetic energy. For μLEED, an aperture was used to selectively illuminate an area with 400 nm diameter from which the μLEED-pattern was obtained. During acquisition of μLEED-patterns, spots that arise from facets normal to the incoming electron beam are stationary as different electron energies are tuned in[6] (in difference to conventional LEED) and can thus be assigned to a NW facet being oriented parallel to the substrate.

Theoretical calculations:

For the theoretical determination of the band gap and the band alignment of the InAs polytypes, we performed density functional theory (DFT) calculations of bulk Zb, bulk Wz and of combined Zb/Wz supercells. The latter consisted of a stacking sequence $(ABC)_n(AB)_n$ along the (111) direction, where A, B, and C stand for an InAs bilayer in three different lateral positions. In our calculations, structures with n=3 or n=5 were realized, i.e. either 9 layers of Zb InAs plus 6 layers of Wz InAs, or 15 layers of Zb InAs plus 10 layers of Wz InAs. The structural parameters of these unit cells, as well as the atomic positions, were fully relaxed. For determining the band alignment, we use the average potential either in (111) planes of the Zb or in (0001) planes of the Wz segment as reference, and compare it to the average potential in the corresponding bulk crystals as described in Ref.[7]. In this way, the effect of an atomic-scale electrostatic dipole layer at the Zb/Wz interface is taken into account.

The calculations are performed within the plane-wave approach with the software package VASP.[8] The wave functions are expanded in a plane wave basis set with the kinetic energy cutoff of 250 eV. The projector-augmented-wave method[9] is used to describe the interaction of the electrons with the ionic cores. In the In atoms, the 4d electrons are treated as core electrons.

Spin–orbit coupling is disregarded in our calculations, as it is of the same size in both InAs polytypes (cf. results of Ref. [10]). The HSE06 functional[11] is used to describe the electronic exchange and correlation. The Brillouin zone sampling was achieved by a 25×25×25 k-point-mesh in the first Brillouin zone for Zb and Wz, respectively. For an accurate evaluation of the density of states in the conduction band, the calculations were repeated without charge self-consistency on a denser mesh around the Γ point, followed by a fitting of the band structure and extrapolation to an even denser mesh.

Additionally, DFT calculations of the InAs NW surfaces are carried out. The side facets of InAs NW are modeled by Zb {110} and Wz {11−20} or {10−10} surfaces. The slabs employed in the calculations contain 10 and 12 In–As bilayers, separated by a vacuum with a thickness of 15 Å for Zb and Wz surfaces, respectively. The dangling bonds at the backside of the substrate are saturated using hydrogen atoms with fractional charges. Surface band structures are obtained by performing self-consistent calculations in the local density approximation (LDA),[12] using a 12×12 k-point mesh to sample the surface Brillouin zone, followed by calculations of the band energies along the high-symmetry lines of the surface Brillouin zone. To obtain the electronic density of states at the surface, the atomic geometry of the LDA calculations is used as a starting point for a HSE06 calculation with fixed geometry. The HSE06 functional gives a more realistic surface band gap which can be compared to the bulk band gap.

Values of band edges without correction for TIBB:

Band edges as retrieved from the plots in Fig. 3 before correcting for tip-induced band bending: $E_{v,\{10-10\}} = -0.375$ eV, $E_{c,\{10-10\}} = 0.06$ eV, $E_{v,\{110\}} = -0.425$ eV, $E_{c,\{110\}} = -0.012$ eV,

$E_{v,\{11-20\}} = -0.470$ eV, $E_{c,\{11-20\}} = -0.015$ eV. The precision in determining the absolute values of the band edges in this way is generally believed to be ±0.03 eV[2]; relative differences are however expected to be more accurate.

Turning our attention briefly to the {10−10} facet, we find a band gap after TIBB correction of 370 meV, 20 meV smaller than what was found for the {11−20}-type facet, and a different band alignment. The discrepancy in Wz band gap energy can be explained by our lack of knowledge of the local tip-sample settings (*e.g.* varying contact potential) and therefore not being able to simulate the TIBB correctly for the {10−10}-type facet. The vacuum energy for the {10−10}-type facet can be trusted though as it is measured by PEEM.

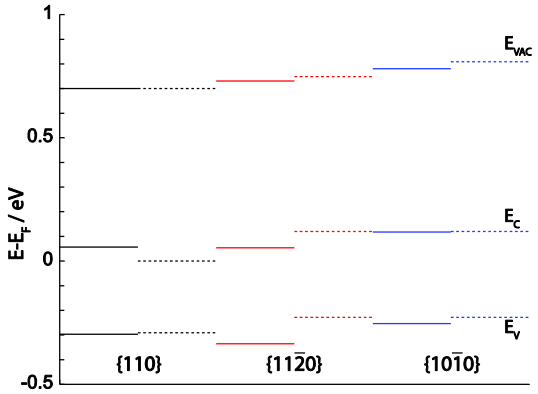

Figure S1. Experimental (solid lines) and theoretical (dashed lines) data from Table 1 shown in a graph. The experimental STM data has been corrected for TIBB. The vacuum level for the {110}-type facet is arbitrarily set to 0.7 eV above the Fermi level for ease of viewing.

References:

1. Magnusson, M. H.; Deppert, K.; Malm, J.-O.; Bovin, J.-O.; Samuelson, L. Size-Selected Gold Nanoparticles by Aerosol Technology. *Nanostructured Materials* **1999**, *12*, 45-48.
2. Feenstra, R. M. Tunneling Spectroscopy of the (110)-Surface of Direct-Gap III-V Semiconductors. *Phys Rev B* **1994**, *50*, 4561-4570.
3. Martensson, P.; Feenstra, R. M. Geometric and Electronic-Structure of Antimony on the Gaas(110) Surface Studied by Scanning Tunneling Microscopy. *Phys Rev B* **1989**, *39*, 7744-7753.
4. Lang, N. D. Spectroscopy of Single Atoms in the Scanning Tunneling Microscope. *Phys Rev B* **1986**, *34*, 5947-5950.
5. Feenstra, R. M.; Stroscio, J. A.; Fein, A. P. Tunneling Spectroscopy of the Si(111)2 × 1 Surface. *Surf Sci* **1987**, *181*, 295-306.
6. Hawkes, P. W.; Spence, J. C. H. *Science of Microscopy*. Springer: 2007.
7. Van de Walle, C. G.; Martin, R. M. Theoretical Calculations of Heterojunction Discontinuities in the Si/Ge System. *Phys Rev B* **1986**, *34*, 5621-5634.
8. Kresse, G.; Furthmüller, J. Efficient Iterative Schemes for ab initio Total-Energy Calculations Using a Plane-Wave Basis Set. *Phys Rev B* **1996**, *54*, 11169-11186.
9. Blöchl, P. E. Projector Augmented-Wave Method. *Phys Rev B* **1994**, *50*, 17953-17979.
10. Belabbes, A.; Panse, C.; Furthmüller, J.; Bechstedt, F. Electronic Bands of III-V Semiconductor Polytypes and their Alignment. *Phys Rev B* **2012**, *86*, 075208.
11. Heyd, J.; Scuseria, G. E.; Ernzerhof, M. Hybrid Functionals Based on a Screened Coulomb Potential. *J Chem Phys* **2003**, *118*, 8207-8215.
12. Perdew, J. P.; Zunger, A. Self-Interaction Correction to Density-Functional Approximations for Many-Electron Systems. *Phys Rev B* **1981**, *23*, 5048-5079.